Novel non-transposable-element regulation patterns of KZFP family reveal new drivers of its rapid evolution

Pan Shen[1, #], Qijian Zheng[1, #], Aishi Xu[1, 2], Junhua Liu[1], Yushan Hou[1], Chao Gao[1], Chunyan Tian[1, *], Fuchu He[1, *], Dong Yang[1, *]

[1] State Key Laboratory of Proteomics, Beijing Proteome Research Center, National Center for Protein Sciences (Beijing), Beijing Institute of Lifeomics, Beijing 102206, China

[2]Animal Sciences College of Jilin University. Changchun, 130062, China.

[#] These authors contributed equally to this work

[*] Corresponding authors: Email: yangdongbprc@163.com, hefc@nic.bmi.ac.cn or tianchunyan@mail.ncpsb.org.

Abstract

One striking feature of the large KRAB-containing zinc finger protein (KZFP) family is its rapid expansion and divergence since its formation about 400 million years ago. However, the evolutionary characteristics of KRAB domains, C2H2 zinc fingers and the full protein of KZFPs have not been fully analyzed. As for the drivers of the rapid evolution, it's partly due to their coevolution with transposable elements (TEs). But their diverse functions besides inhibiting TEs suggest other reasons exist. Here we address these two issues by the systematic analysis of the divergence time and diversification pattern of KZFPs at three aspects and the functional analysis of the potential target genes besides TEs. We found that old-zinc-finger-containing KZFPs tend to have varied and disordered KRAB domains, indicating there are two ways of the evolution of KZFPs, including the variation of KRAB domains and the diversification of zinc fingers. Among them, the divergence of zinc fingers mainly contributes to the rapid evolution of KZFPs. Thus, we mainly focused on the functional requirements of the evolution of zinc fingers. Different from the classical regulation pattern of this family, we found and experimentally confirmed that KZFPs tend to bind to non-TE regions and can positively regulate target genes. Although most young genes tend to be with a low expression level, young-zinc-finger-containing KZFPs tend to be highly expressed in early embryonic development or early mesoderm differentiation, indicating their particular evolutionarily novel functional roles in these two processes. We further validated a young KZFP, ZNF611, can bind to non-TE region of STK38 gene and positively regulates its expression in ESCs. The emergence of new sequence in STK38 promoter may drive the evolution of zinc fingers in ZNF611. Finally, we proposed a 'two-way evolution model' of KZFP family.

39 **Key words:** KZFP, evolutionary divergence time, target gene, non-TE, functional
40 constraint

41

Introduction

KRAB domain-containing zinc finger protein (KZFP) family, the largest family of transcription factors in mammalian (Nowick et al., 2011), has 363 member genes in human genome. Generally, KZFP contains a KRAB domain and a C-terminal C2H2 zinc finger array with DNA-binding potential (supplementary fig. 1). Both C2H2 zinc finger and KRI (KRAB Interior) motif, which is the ancestor of KRAB domain (Birtle & Ponting, 2006), are old motifs, appearing widely across animals, plants and fungi. However, these two kinds of motifs did not appear in the same protein during the lengthy process of evolution until their 'marriage' in the last common ancestor of coelacanths and tetrapods (Imbeault, Helleboid, & Trono, 2017) about 400 million years ago. After that, the KZFP family expanded and diverged quickly especially during the evolution of mammalian.

The phenomena of the rapid evolution of KZFP family include three aspects: (1) The strong specificity of KZFP family across species. Lots of species-specific KZFP genes were reported in human, chimpanzee and other species (Huntley et al., 2006; Imbeault et al., 2017; Nowick et al., 2011; Thomas & Schneider, 2011). (2) The quick expansion of the number of KZFP member gene and C2H2 zinc finger motif in a KZFP. The number of KZFP genes (Emerson & Thomas, 2009; Looman, Abrink, Mark, & Hellman, 2002; Nowick et al., 2011) and the average zinc finger number per KZFP (Emerson & Thomas, 2009) in mammalian are much more than those in birds, reptiles and amphibians. (3) The rapid divergence of full protein sequence or C2H2 zinc finger motif among KZFP orthologs. Some studies revealed that phylogenetically specific KZFP genes are under strong positive selection (Emerson & Thomas, 2009; Looman et al., 2002). The specificity of the binding sequence is depended mainly on three key amino acids within each zinc finger (at positions 6, 3 and -1 of the C2H2

helix) (supplementary fig. 1), and the amino acid at position 2 which contacts the secondary strand (Ecco, Imbeault, & Trono, 2017; Emerson & Thomas, 2009). It was revealed that the key amino acids in C2H2 zinc fingers were also of great diversity among different species (Emerson & Thomas, 2009; Hamilton et al., 2006; Imbeault et al., 2017). In a word, KZFP family expanded and diversified rapidly during the evolution of mammalian lineage.

There are numerous studies focusing on the causes about rapid evolution of KZFP family. The previous studies found that KZFP can inhibit endogenous retroelements during early embryonic development (G. Wolf et al., 2015) and embryonic stem cells (D. Wolf & Goff, 2009), even in adult tissues (Ecco et al., 2016). Furthermore, a lot of data indicated that there is a coevolution between zinc fingers in KZFP family and transposable elements (TEs) (Ecco et al., 2017; Jacobs et al., 2014; Thomas & Schneider, 2011). There are two co-evolution models: (1) the arms race model (Jacobs et al., 2014), in which KZFP proteins unremittingly suppress the invasion of rapidly mutating TEs via changing the key amino acids of zinc fingers; and (2) the domestication model (Ecco et al., 2017; Pontis et al., 2019), in which KZFPs regulate domestication of TEs instead of restraining the transposition potential of TEs. Thus, the regulation of TEs is an important driver for rapid evolution of the KZFP family. However, KZFPs also have many other functions besides repressing TEs (Baudat et al., 2010; Grey et al., 2011; Grey, Baudat, & de Massy, 2018; Guo et al., 2009; Kang et al., 2012; X. Li et al., 2008; Patel et al., 2018; Riso et al., 2016; Takahashi et al., 2019; D. Yang et al., 2013), suggesting the rapid evolution of zinc fingers in KZFP family may be also related to their special functions besides repressing TEs.

Here, we focused on the deep and systematic analysis of the evolutionary

characteristics of KZFP family and the reasons for the rapid evolution of this family. By identifying the evolutionary features of the KRAB domains, zinc fingers and the full protein of KZFPs, and analyzing the functions of target genes besides TEs, this study provides new understandings about the rapid evolution of KZFP family.

Results

Comparison of the divergence time of the full sequence, KRAB domain and zinc fingers in KZFPs

In order to fully describe the evolutionary characteristics of KZFP family, the evolutionary divergence time of each member of the human KZFP family was calculated. For each KZFP, the full protein sequence, KRAB domain and the key amino acids of zinc fingers were searched for its orthologs across species and the divergence time was determined according to the last common ancestor of the species containing its orthologs (see Method section for detail). Then the distribution pattern of these three types of divergence time was explored. Firstly, by directly comparing the divergence time distribution of the three type of divergence times, we found that, in general, the divergence times of zinc fingers are significantly later than the other two types of divergence times (fig. 1A, supplementary fig. 2A). Subsequently, we compared the difference value of divergence time between any two types of divergence times of each KZFP. KRAB divergence time is much earlier than the divergence time of full protein sequence in 40.7% of KZFPs, and is later in 31.6% of KZFPs (fig. 1B). Zinc finger divergence time is later than the divergence time of full protein sequence in 49.0% of KZFPs and is later than KRAB domain divergence time in 59.1% of KZFPs. On contrast, the divergence time of zinc finger is earlier than the divergence time of full protein sequence only in 4.8% of KZFPs and is earlier than KRAB domain divergence time only in 10.2% of KZFPs. These results showed that

about half of KZFPs are much younger when they are evaluated by the divergence time of zinc fingers than by that of the full protein sequences or KRAB domains. The more newly emerged zinc fingers reveal that the rapid evolution of KZFPs in mammalian is mainly reflected in the rapid evolution of zinc fingers of them.

Interestingly, the three types of divergence time are all the most at the grade of Eutheria (105 million years ago, Mya). There are 133, 188, 155 KZFPs belonging to this grade of divergence time of the full protein sequence, KRAB domain and zinc finger respectively (supplementary fig. 2A&2B). Their intersection and union are 72 and 258 respectively. This result indicates that there are a large number of KZFPs originating in the common ancestor of eutherians. This may be related to the special traits in this clade. Compared with the other mammalians, such as marsupials and monotremes, eutherians have relatively long gestation periods during embryonic development (Behringer, Eakin, & Renfree, 2006), in which the KZFPs with the age of 'Eutheria' may play important roles (Nowick, Carneiro, & Faria, 2013).

The diversification pattern of KRAB domains and zinc fingers in human

The rapid and frequent divergence of the sequence of KZFPs led to the diversification of KZFP members in the current existing species. To characterize the outcome of the evolution of KZFP family in human genome, the diversification patterns of the KRAB domains and the key amino acids of zinc fingers were analyzed. Through multiple sequence alignment of all human KRAB-A box sequences, we found that a cluster of 35 KZFPs have variant KRAB domains compared with other KZFPs (fig. 2A). We then supposed that the KRAB domains of these 35 KZFPs may also have special structural characteristics. The structural disorder ratio of the KRAB domains was compared between these 35 KZFPs and others. As the result, these 35 KRAB domains are significantly more disordered than the other 328 KRAB domains

(fig. 2B). Disordered protein domains tend to have diverse structural conformations, and then have diverse interacting partners and functions (Csizmok, Follis, Kriwacki, & Forman-Kay, 2016; Mosca, Pache, & Aloy, 2012). Thus, we inferred that the KRAB domains in this special cluster may have diverse interacting partners besides KAP-1, the universal and canonical partner of KRAB domain. This result is consistent with a previous study (Helleboid et al., 2019) which showed that the variant KRAB box may mediate non-canonical interactions. We further investigated the distribution of the divergence time of these 35 KRAB domains. Compared with all the human KRAB domains, these 35 KRAB domains tend to be old (Amniota − Mammalia) or young (Euarchontoglires − Catarrhini), but are under-represented in middle-aged class (Theria − Boreoeutheria) (fig. 2A, supplementary fig. 2C). Even so, the middle-aged KRAB domains still account for the largest proportion in this variant cluster. This phenomenon suggests that these variant KRAB domains were formed gradually, rather than concentrated in a specific period of evolution.

When the divergence time of zinc fingers was considered, among these 35 KZFPs, 23 of them (65.7%) contain old zinc fingers (the divergence time is over 159 Mya) (fig. 2A). If we calculated using the number of KZFPs containing old zinc fingers as the denominator, 67.6% (23/34) of KZFPs with old zinc fingers contain variant KRAB domains (fig. 2A). These two results revealed that there is a large intersection between the old-zinc-finger-containing KZFPs and the KZFPs with a variant KRAB domain. In other words, KZFPs with evolutionarily conserved zinc fingers tend to have a variant KRAB domain. This suggest there are two different ways for the evolution of KZFPs. One is the divergence of key amino acids in zinc fingers (that is, KZFPs containing young zinc fingers). 90% of the KRAB domains in

these KZFPs are completely structured (fig. 2C), suggesting that they have a single and unchangeable function execution pattern and constantly interact with a specific co-factor (such as KAP-1). In another evolutionary path, the key amino acids in the zinc fingers are conserved (that is, KZFPs containing old zinc fingers). However, the KRAB domains of these KZFPs are variable and tend to be disordered (fig 2C), suggesting that their KRAB domains are versatile, interacting with multiple proteins.

Besides KRAB domains, C2H2 zinc finger motifs and the non-domain regions of KZFPs with variant KRAB domains (supplementary fig. 3A-3C) or old zinc fingers (supplementary fig. 3D & 3E) are more disordered than those in other KZFPs (supplementary result). But after all, KZFPs with variant KRAB domains or old zinc fingers are only a small part. For the entire KZFP family, KRAB domains tend to be completely structured although they are absolutely young domains (supplementary fig. 3F&3G; supplementary result). Furthermore, at protein level, KZFPs are also highly structured, suggesting that most of KZFPs are monotonous and unchangeable in structural conformation and functional mechanism (supplementary fig. 4; supplementary table 1; supplementary result).

In order to analyze the diversification pattern of zinc figures in human, the similarity of zinc fingers based on three key amino acids within each zinc finger in human KZFPs were calculated. As the result, the similarity between most zinc finger pairs are very low (fig. 2D, supplementary table 2), only 153 (0.23%) KZFP pairs have similarity value over 0.6 (fig. 2E). Furthermore, by identifying the homologous relationship of human KZFPs, we found that only 121 (33.3%) KZFPs belong to 44 paralogous gene groups, while 242 (66.7%) KZFPs are singletons (fig. 2F). These results indicate that the key amino acids in KZFP zinc fingers are diverse.

Overall, from the above results we can infer that the most remarkable

191 evolutionary characteristics of KZFPs are as follows: although there are two ways of
192 evolution for this family, that is KRAB variation or zinc finger variation, most of
193 KZFPs belong to the 'zinc finger variation' evolution class. These KZFPs have
194 relatively young and diverse zinc fingers, suggesting their targeting sequences may
195 also evolved quickly, which acted as drivers for the quick evolution of zinc fingers.

196 **KZFPs tend to bind to non-TE regions in exon and promoter**

197 In order to analyze the functional differences of KZFPs with different
198 evolutionary features and explore the reasons for the rapid evolution of the KZFP
199 family, the target gene information of KZFP should be investigated. To this end, we
200 collected ChIP-seq or ChIP-exo data of 262 KZFPs (supplementary file). An
201 important function of KZFPs is to bind and inhibit transposable elements (TEs),
202 especially retroelements (Ecco et al., 2017; P. Yang, Wang, & Macfarlan, 2017), and
203 there is a co-evolution model between KZFPs and TEs (Jacobs et al., 2014; Thomas &
204 Schneider, 2011). To comprehensively analyze the genome-wide TE-binding tendency
205 of KZFPs, we analyzed the KZFP binding sites in various regions of the genome. For
206 a KZFP, if over half of the KZFP peaks binding to TEs in a region, the KZFP is
207 identified as the KZFP tending to bind to TEs in this region and *vice versa*. Based on
208 this standard, we found over half of KZFPs tend to bind to non-TE regions in genome
209 (fig. 3A; supplementary table 3). And more interestingly, around 90% of KZFPs tend
210 to bind to non-TE regions in exon, UTR and promoter (fig. 3A; supplementary table
211 3). However, according to the result of two previous studies, KZFPs tend to bind to
212 TEs in genome (Helleboid et al., 2019; Imbeault et al., 2017). We found that main
213 reason for this difference is the different versions of MACS program used in the
214 ChIP-seq data processing (supplementary results; supplementary table 4).
215 Furthermore, we confirmed that MACS2 used in this study is more accurate than

MACS1.4 used in the previous studies (Helleboid et al., 2019; Imbeault et al., 2017), indicating that our conclusion that KZFP tend to bind to non-TE regions is valid (supplementary results; supplementary fig. 5).

Since there is a coevolution phenomenon between the zinc fingers of KZFP and the sequence of TE (Ecco et al., 2017; Jacobs et al., 2014; Thomas & Schneider, 2011), we assumed that there may be a tendency that KZFPs with younger zinc fingers may tend to bind to TEs. To test this speculation, we analyzed the binding bias of KZFPs with different zinc finger divergence times. Within the whole genome, it is obvious that KZFPs with younger zinc fingers tend to bind to TEs (fig. 3B & supplementary fig. 6).

We next sought to clarify the detailed functions of KZFPs which bind to non-TE regions. Based on KZFP ChIP-seq or ChIP-exo data, all of the PCGs were classified into three categories: noKZFP_PCGs, KZFP-TE_PCGs and KZFP-nonTE_PCGs (fig. 3C). We found that the biological functions of these three types of PCGs were obvious different. Interestingly, the development related processes were specifically over-represented in KZFP-nonTE_PCGs (fig. 4D), and KZFP-TE_PCGs were with higher tolerance to functional variations than KZFP-nonTE_PCGs (fig. 3E). Moreover, KZFP-TE_PCGs and KZFP-nonTE_PCGs are under higher purifying selection pressure than noKZFP_PCGs (fig. 4F). These results revealed that KZFP-nonTE_PCGs are of greatest functional essentiality among the three types of PCGs, indicating the functions regulated by KZFPs via binding to non-TE regions are very important.

KZFP genes encoding young zinc fingers tend to have higher expression level in early embryonic development and the ESC differentiation into mesoderm

The preceding analyses are not related to the expression of KZFPs in certain

241 spatio-temporal states. The investigation of the expression level of KZFPs in different
242 spatio-temporal states is of great importance to understand their functions. In general,
243 old genes often have higher expression level than young genes (Cardoso-Moreira et
244 al., 2019). To verify whether the divergence time of the KZFP genes is correlated to
245 their expression level, we explored the relationship between the evolutionary
246 divergence time (full protein divergence time, KRAB domain divergence time and
247 zinc finger divergence time) and gene expression level. Full protein divergence time is
248 positively correlated with gene expression level for both TFs and other PCGs in
249 almost all samples, and for C2H2-ZFPs in part of samples. However, this correlation
250 for KZFPs was not significant in all samples. Interestingly, there was a negative
251 correlation between zinc finger divergence time and expression level of KZFPs in
252 early embryonic development and early mesoderm differentiation (fig. 4A;
253 supplementary table 5), such as ZNF90, ZNF611 and ZNF814 (fig. 4B). In other
254 words, in these samples, KZFPs with young zinc fingers have higher gene expression
255 level, suggesting that younger-zinc-finger-containing KZFPs may play important roles
256 in early embryonic development and early mesoderm differentiation.

257 **KZFPs can positively regulate target genes by binding to non-TE regions in**
258 **endoderm or mesoderm differentiation**

259 The data of chromatin accessibility, such as ATAC-seq data, can improve the
260 predictability of *in vivo* transcription factor (TF) binding sites (Keilwagen, Posch, &
261 Grau, 2019; H. Li, Quang, & Guan, 2019). Since transcription activators
262 predominantly bound in accessible chromatin (Thurman et al., 2012), ATAC-seq data
263 was mainly used for the prediction of TF binding sites mediating positive regulation.
264 Interestingly, the peaks of KZFP ChIP-seq overlapping with non-TE regions were
265 more likely to exist in open chromatin region in ESC than those overlapping with TEs

(fig. 5A).

In order to obtain high-credibility target genes of KZFPs, gene expression data (RNA-seq), ChIP-seq, ChIP-exo and ATAC-seq data were combined together to screen the target genes positively regulated by KZFPs in endoderm or mesoderm differentiation (fig. 5B). In total, we screened 4,116 target genes positively regulated by 112 KZFPs during ESCs differentiation to endoderm, and 2,490 target genes positively regulated by 76 KZFPs during ESCs differentiation to mesoderm. Of the two target gene sets mentioned above, 86.1 % and 83.8 % are KZFP-nonTE PCGs respectively. To verify the reliability of this prediction, ZNF202, ZNF383 and ZNF589 from endoderm differentiation and ZFP14, ZNF554 and ZNF565 from mesoderm differentiation were randomly chosen for the experimental validation. Interestingly, they positively regulated their target genes in ESCs but not in HEK293T cells (supplementary fig. 7A-7E; supplementary results). This could be further confirmed by the status of chromatin accessibility of the target genes in these two cell lines (supplementary fig. 7F; supplementary results). Further analysis of binding sites of 262 KZFPs in ESCs and HEK293T cells, we also found that many regions bound by KZFPs are in accessible chromatin in ESCs, while in HEK293T cells they are in inaccessible chromatin (supplementary fig. 8). These results indicated that KZFPs can play positive regulatory roles in particular biological states.

According to the traditional understanding of KZFP functions, most of KZFPs silenced TEs and also repressed the neighboring gene expression at TEs (Jacobs et al., 2014; Oleksiewicz et al., 2017; P. Yang et al., 2017). Previously, some studies also found that part of KZFPs can positively regulate target genes. For example, Schmitges *et al.* found 31 KZFPs can interact with at least one activator and it was further confirmed that ZNF554 can positively regulate the expression of target genes

(Schmitges et al., 2016). Chen *et al.* found that ZFP30 positively regulated the target genes by binding to TE-derived enhancers (Chen et al., 2019). However, it is still unclear whether KZFPs may play positive regulatory roles by binding to non-TE regions. Here, we firstly report that there are a large number of target genes positively regulated by KZFPs via binding to non-TE regions in certain spatiotemporal states. These new findings expand our understanding of the functional characteristics of the KZFP family.

To understand the detailed functions of target genes positively regulated by KZFPs, we analyzed the regulatory functions of KZFP-TE_PCGs and KZFP-nonTE_PCGs in these two differentiation processes. Interestingly, we found KZFP-nonTE_PCGs specifically tend to participate in the functions closely related to the development of corresponding embryo layer in both endoderm differentiation and mesoderm differentiation, such as pharyngeal system development (supplementary fig. 9A) and heart development (fig. 5C). These results indicate that KZFPs play important roles in the differentiation of ESCs to endoderm or mesoderm via regulating target genes by binding to non-TE regions.

From the perspective of functional essentiality, KZFP-TE_PCGs have higher tolerance than KZFP-nonTE_PCGs in both differentiation of endoderm (supplementary fig. 9B) and mesoderm (fig. 5D). Moreover, KZFP-TE_PCGs are under lower purifying selection pressure than KZFP-nonTE_PCGs in endoderm differentiation (supplementary fig. 9C), while there is no significant difference in mesoderm differentiation (fig. 5E). These results further confirmed that KZFP-nonTE_PCGs are under stronger functional constraint and selection pressure, consistently indicating that binding to the non-TE regions in promoters is an important regulatory mechanism for KZFPs and the target genes that regulated by

316 KZFPs binding to non-TE regions are more essential.

317 **The emergence of new sequence in STK38 promoter may drive the evolution of**
318 **zinc fingers in ZNF611**

319 As described in the preceding section, some KZFPs containing young zinc
320 fingers highly expressed in early mesoderm differentiation (fig. 4). To validate the
321 functional roles of these young-zinc-finger-containing KZFPs in mesoderm
322 differentiation, the key KZFPs that may play important roles were selected and the
323 validation experiments were conducted. Combined zinc finger divergence time, gene
324 expression in mesoderm differentiation and the known functional annotations of
325 KZFP target genes, ZNF611 and its target genes bone morphogenetic protein receptor,
326 type II (BMPR2) and serine/threonine kinase 38 (STK38) were selected to do the
327 validation experiments. BMPR2 is a transmembrane serine/threonine kinase that binds
328 BMP2 and BMP7 in association with multiple type I receptors, including
329 BMPR-IA/Brk1, BMPR-IB, and ActR-I (Liu, Ventura, Doody, & Massague, 1995).
330 STK38 is a member of the protein kinase A (PKA)/PKG/PKC-like family, and STK38
331 can negative regulate of MEKK1/2 signaling (Enomoto et al., 2008). Both BMPR2
332 and STK38 are important in mesoderm differentiation, so we assumed that ZNF611 is
333 involved in mesoderm differentiation by positively regulating BMPR2 and STK38. To
334 test the hypothesis, we first examined the effect of ZNF611's expression level on the
335 mRNA level of BMPR2 and STK38 using quantitative PCR. The overexpression of
336 ZNF611 in the ESC cells increased the mRNA level of *STK38* (fig. 6A). Similarly,
337 when ZNF611 was knockdown with two different siRNA sequences, the mRNA level
338 of *STK38* was decreased as well (fig. 6B).

339 Furthermore, we want to predict and verify the binding site of ZNF611 in the
340 promoter of *STK38* gene. According to ChIP-seq data, ZNF611 can bind to non-TE

region in 5' UTR of STK38 (fig. 6C). ChIP-qPCR analysis was conducted to examining the binding of ZNF611 in non-TE region in 5' UTR of STK38. We overexpressed the flag-tagged ZNF611 and observed an enrichment of non-TE region in 5' UTR of STK38 in ChIPs by using flag antibodies (fig. 6D). These observations indicated that ZNF611 indeed binds to non-TE region in 5' UTR of STK38 and positively regulates STK38 in ESCs, suggesting that ZNF611 can regulate the differentiation of ESC into mesoderm by positively regulating STK38.

We next explored whether the binding sequence in STK38 promoter drives the evolution of key amino acids in zinc fingers of ZNF611. To this end, we collected the key amino acids in the zinc fingers of ZNF611 and other KZFPs in the cluster produced by Imbeault *et al.* (Imbeault et al., 2017). Then the sequences of key amino acids were aligned and the phylogeny tree was generated (fig. 6E). We can see that the key amino acids of ZNF611 are similar with other homologous KZFPs within Catarrhini instead of other Simiiformes, consistent with the zinc finger divergence time determined by Imbeault *et al.* (Imbeault et al., 2017). We predicted the ZNF611 binding motif by RACDE (Najafabadi, Albu, & Hughes, 2015) and found that there was a binding sequence of ZNF611 in 5' UTR of STK38 (fig. 6F). Based on the alignment of the STK38 promoter locus from 21 representative species, we found the ZNF611 binding site in STK38 are highly conserved in Simiiformes (fig. 6G). To further verify the accuracy of the ZNF611 binding site, we cloned a ~1.2-kb DNA fragment upstream of the STK38 transcription start site (TSS) into a pGL3-basic luciferase vector (termed pGL3-STK38-P), containing the described ZNF611 binding motif. We also generated deletion lacking the ZNF611 binding motif (pGL3-STK38-ΔP) (fig. 6H). The ZNF611 overexpression dose-dependently increased the luciferase activity of pGL3-STK38-P, but not the pGL3-STK38-ΔP

reporter (fig. 6I). These results suggested there was a co-evolution between the binding sequence in the 5'UTR of STK38 and the zinc fingers of ZNF611: The new sequence in STK38 appeared in the common ancestor of simiiformes, and then (about 14 million years later) the zinc fingers of ZNF611 evolved to adapt to the emergence of the new sequence. Therefore, there was a change in key amino acids in zinc fingers of ZNF611 in the common ancestor of catarrhini.

Discussion

In this study, we tried to comprehensively characterize the evolutionary features of KZFPs by the analysis of the divergence time and diversification pattern of KRAB domains, zinc fingers and the full protein of KZFPs. We then explored the functional features of the target genes of KZFPs with different ages, so as to answer the question why KZFP family evolved so fast. We found that: (1) the rapid evolution of KZFPs in mammalian is mainly reflected in the rapid evolution of zinc fingers of them. (2) KZFPs with old zinc fingers contain variable and disordered KRAB domains. (3) Different with the previous conclusions (Helleboid et al., 2019; Imbeault et al., 2017), KZFPs tend to bind to non-TE regions, instead of TEs, particularly in exons, and promoters. (4) Different from the classical repression function of KZFPs, we found that, in certain processes, such as ESC differentiation, lots of KZFPs can positively regulate target genes via binding to non-TE regions. (5) Some young zinc-finger-containing KZFPs (e.g. ZNF611) are highly expressed in early embryonic development and early mesoderm differentiation. After experimental verification, we found ZNF611, which contains young zinc fingers, binds to non-TE region in 5' UTR of STK38 and positively regulates its expression in ESCs, and importantly, the emergence of new sequence in STK38 promoter may drive the evolution of zinc fingers in ZNF611. These results indicate that the KZFPs containing young zinc

391 fingers can positively regulate genes and play important roles in the differentiation of
392 ESC into mesoderm by binding to non-TE regions, suggesting that the function of
393 binding to non-TE regions may be one of the drivers for rapid evolution of zinc
394 fingers in KZFPs. Moreover, STK38 was up-regulated in differentiation of human
395 ESCs into mesoderm, while Stk38 was down-regulated in differentiation of mouse
396 ESCs into mesoderm (supplementary fig. 10), suggesting that there is a new
397 regulation (that is, positively regulated by ZNF611) of STK38 in differentiation of
398 human ESCs into mesoderm. Overall, these findings show that binding to non-TE
399 regions is one of the important ways for KZFPs to greatly contribute to the formation
400 and evolution of gene regulatory networks.

401 Based on our results, combining with the conclusions of existing researches
402 (Ecco et al., 2017; Helleboid et al., 2019), we proposed a new KZFP family evolution
403 model: 'two-way evolution model' (fig. 7). The evolution of the KZFP family mainly
404 includes two directions. One is the divergence of key amino acids in zinc fingers (that
405 is, KZFPs containing young zinc fingers), adapting to the changes of the target sites
406 (such as TEs reported in previous studies, or non-TE regions revealed by this study).
407 Almost all of the KRAB domains in these KZFPs are completely structured and the
408 whole protein of these KZFPs also are relatively highly structured, suggesting that
409 they have a single and unchangeable function execution pattern and constantly
410 interact with a specific co-factor (such as KAP-1). In another evolutionary path, the
411 key amino acids in the zinc fingers are conserved (that is, KZFPs containing old zinc
412 fingers), and their target sites are also conserved. However, the KRAB domains of
413 these KZFPs are variable and tend to be disordered, suggesting that their KRAB
414 domains are versatile, interacting with multiple proteins. Therefore, these KZFPs can
415 play diverse roles.

Materials and Methods

The identification of members in KZFP family, C2H2-ZFP proteins and TFs in *Homo Sapiens*

The *homo sapiens* protein sequences were downloaded from Ensembl release 83 (Zerbino et al., 2018), and the HMM file of KRAB domain and zf-C2H2 domain were download from Pfam v29.0 (Finn et al., 2010). The KZFPs and C2H2-ZFPs were filtered using HMMER v3.1b2 (Eddy, 2009). The validation of transcription factors was based on DBD (DNA-binding domain) transcription factor database (Kummerfeld & Teichmann, 2006) and Ref. (Ravasi et al., 2010).

The definition of the divergence time of the full protein sequence, KRAB domain and zinc finger of KZFPs

The divergence time of the full protein sequence was inferred according to the homology information from Ensembl Compara (Herrero et al., 2016; Vilella et al., 2009). To identify the divergence time of KRAB domain in human KZFPs, protein sequences of 80 species from 80 genera in deuterostomia were downloaded from Ensembl database (supplementary table 6). KRAB domains in 80 species were identified by HMMER v3.1b2 (Eddy, 2009). BLSATP was used to calculate the homology between human KRAB domains and KRAB domains in other 79 species. The hits with the identity and the percentage of the matched sequence in query or subject sequence above 80% were selected as homologous KRAB domains. The KRAB domain divergence time of each human KZFP was determined based on the species with farthest evolutionary distance from human in all species containing the homologous KRAB domains. The divergence times of KZFP zinc finger were inferred according to the similarity between the key amino acids in zinc-fingers (Imbeault et al., 2017). Evolutionary distance between *Homo Sapiens* and other 79 species were

441 estimated by TimeTree (Kumar, Stecher, Suleski, & Hedges, 2017). The divergence
442 time values of full protein sequence, KRAB domain and zinc fingers of KZFPs are
443 available in supplementary table 7.

444 **The phylogenetic analysis**

445 Sequence alignments were performed using ClustalX (version 2.1) with default
446 parameters (Larkin et al., 2007), and the phylogenetic tree (neighbor-joining tree) was
447 constructed using MEGAX (Kumar, Stecher, Li, Knyaz, & Tamura, 2018) with
448 default parameters.

449 **The zinc finger similarity between each KZFP pairs in *Homo Sapiens***

450 The zinc finger similarity between each KZFP pairs was calculated according to the
451 method described previously (Imbeault et al., 2017). Briefly, similarity between two
452 zinc finger arrays was defined as sharing the same three amino acids at the
453 DNA-contacting residues, allowing up to one replacement by a related amino acid (as
454 defined by Blosum62). To identify paralogs of human KZFPs based on zinc fingers: 1)
455 for the KZFP which containing 5 or more zinc fingers, the threshold similarity score
456 of 60% and common zinc-fingers of 5 between any two zinc-finger arrays were
457 selected; for the KZFP which containing 4 or less zinc fingers, a threshold similarity
458 score of 100% between any two zinc-finger arrays was selected.

459 **The disorder scores of proteins and domains**

460 *Structural disorder ration (SDR):* The longest protein encoded by each gene was
461 selected as the representative protein for subsequent analyses. IUPred (Dosztanyi,
462 2018) was used to obtain the disorder score of each amino acid in a protein or domain.
463 The disorder rate of a protein is the ratio of the number of disordered amino acids (the
464 disorder score is greater than 0.5) to the total number of amino acids. According to
465 SDR values, proteins can be divided into four classes: completely structured (SDR =

0), highly structured (0 < SDR ≤ 10 %), relatively disordered (10 % < SDR ≤ 30 %), and highly disordered (30 % < SDR ≤ 100 %).

Consecutively disordered region number (CDRN): 1) for the domains or proteins which are longer than 50 aa, a CDR consists of 20 or more consecutively disordered amino acids; 2) for the domains which are shorter than 50 aa, a region containing consecutively disordered residues exceeding 40% of all domain residues is considered to be a CDR.

RNA-Seq data analysis.

The RNA-Seq data was downloaded from GEO and ArrayExpress database (Supplementary file 1). The reads were mapped to the human genome build GRCh38 (hg38) using Salmon v0.11.0 (Patro, Duggal, Love, Irizarry, & Kingsford, 2017). Isoform expression levels were calculated as transcripts per kilobase of exon model per million mapped reads (TPMs) and read counts using Salmon v0.11.0 (Patro et al., 2017), and gene expression levels were calculated by tximport (Soneson, Love, & Robinson, 2015).

ChIP-seq, ChIP-exo and ATAC-seq data analysis.

The ChIP-seq, ChIP-exo and ATAC-seq data was downloaded from GEO DataSets and ENCODE (Consortium, 2012) (Supplementary file 1). The reads were mapped to the human genome build GRCh38 using HISAT2 (Kim, Langmead, & Salzberg, 2015). Duplicate reads, which often represent PCR amplification artifacts, were removed using SAMtools version 1.3. We used MACS version 2.1.0 (Feng, Liu, Qin, Zhang, & Liu, 2012; Zhang et al., 2008) with the 'keep-dup all' parameter, which is recommended for ChIP-exo as genuine reads can accumulate on a few positions following exonuclease digestion (Imbeault et al., 2017). We filtered out peaks that would meet any of these criteria: $P < 1\times10^{-16}$. The transcription start sites (TSSs) were

retrieved from Ensembl release 83. The region from +2,000 bp to -500 bp of their nearest TSS were annotated as promoters (Tsankov et al., 2015). The genes whose promoters were overlapped with KZFP peaks were considered to be potential KZFP target genes.

TE information

The TEs were obtained with the RepeatMasker track (Smit, AFA, Hubley, R and Green, P. RepeatMasker Open-3.0.1996–2010 http://www.repeatmasker.org) (Jurka, 2000) from the hg 19 and hg38 genome assembly.

Screening process of KZFP target genes

If the promoter region of a PCG is bound by a KZFP, the PCG is considered as a possible target gene of the KZFP. Genes which were expressed at least in one stage (ESC, endoderm or mesoderm) were included in the following analysis. Differentially expressed genes from ESCs to endoderm or mesoderm were screened according to the fold changes in four data sets (up-regulated trend: The fold change is greater than 1.1 at least in three data sets; down-regulated trend: The fold change is less than 0.91 at least in three data sets). Chromatin accessibility data in ESCs, endoderm and mesoderm were used to filtrate the KZFP target genes: 1) if a KZFP peak bind to a promoter of PCG with accessible chromatin in both ESC and endoderm or mesoderm, the expression trend between KZFP gene and PCG should be same; 2) if a KZFP peak bind to a promoter of PCG with accessible chromatin only in ESC, both KZFP gene and PCG should be down-regulated; 3) if a KZFP peak bind to a promoter of PCG with accessible chromatin only in endoderm or mesoderm, both KZFP gene and PCG should be up-regulated. The potential target genes of KZFPs in differentiation from ESCs to endoderm or mesoderm were listed in supplementary table 8.

The over- or under-representation analysis

This was performed using the method as previously described (D. Yang et al., 2012). Briefly, we first selected genes with BP term annotations. Subsequently, we filtered genes expressed during the differentiation of ESC into endoderm or mesoderm as the background. To analyse the over- or under-representation strengths of genes in each class relative to the background, we used the method based on hypergeometric distribution. The over- or under-representation strengths of each class were represented by -log (*p*) or log (*p*).

Retrieving the metrics of functional constraint and evolutionary rate measurements

We characterized KZFP target genes using three different measurements of functional constraint: (1) the residual variation intolerance score (RVIS); (2) the probability of being intolerant to loss-of-function mutations (pLI); and (3) the selection against heterozygous loss of gene function (S_{het}). We obtained the pLI and RVIS percentile from Ref.(Dickinson et al., 2016) and S_{het} scores from Ref.(Cassa et al., 2017). The number of synonymous substitutions per synonymous site (dS) and the number of nonsynonymous substitutions per nonsynonymous site (dN) between the ortholog pairs of human and chimpanzee were retrieved using BioMart from Ensembl database (Kinsella et al., 2011).

Plasmids and siRNA

ZNF611 mammalian expression vector were constructed by PCR, followed by subcloning into pFLAG-CMV-2 (Sigma). The siRNA was purchased from Gene Pharma (Suzhou, China), and the following sequences were used. siZNF611-1: 5'-GCAGGUCAUCCCUUCAUUGTT-3', siZNF611-2, 5'-GUGUAAUUCACUCCUGUCATT -3'. non-targeting siRNA, 5'-CCAUGUGAACUGGUCACCUTT -3'.

Cell culture and transfections

The HEK293T cells were maintained in DMEM supplemented with 10% fetal bovine serum (Zhejiang Tianhang Biotechnology, Hangzhou, China).

The human ESC line H9 was cultured following the protocols as previously described (Ludwig et al., 2006). Briefly, H9 cells were plated as clumps in feeder-free conditions in six-well plates (Corning) coated with Matrigel (1: 80, BD Biosciences) in mTESR1 medium (Stem Cell Technologies). Gentle Cell Dissociation Reagent (STEMCELL Technologies) was used for passaging (1: 4-1: 7) every 4-7 days when cells reached 70-80% confluency on Matrigel. The differentiated cell clumps were manually removed before passaging to ensure high quality cultures.

When H9 cells reached 70 - 80 % confluency, the clumps were digested into single cells for optimal transfection efficacy. Cells were grown on 12-well plates coated with Matrigel. Single-cell passaging medium by adding Y-27632 (10 μM, Stem Cell Technologies) to mTeSR1 was used for the 1st day of feeder-free culture (Watanabe et al., 2007). Before the transfection, the differentiated cells were manually removed.

Both HEK293T cells and H9 human ESCs were transfected with Lipofectamine 2000 (Invitrogen, CA, USA) according to the manufacturer's instructions.

Quantitative PCR

Total RNA was isolated using Trizol kit (T9424, Sigma-Aldrich). Complementary DNA was synthesized using the cDNA synthesis kit (FSQ-101, TOYOTO, Osaka, Japan) according to the manufacturer’s instructions. Fluorescence real-time RT-PCR was performed using the KAPA SYBR® Faster Universal (KK4601, Biocompare, South San Francisco, CA, USA) and the ABI PRISM 7300 system (Perkin-Elmer, Torrance, CA). PCR was conducted in triplicates and standard deviations representing

566 experimental errors were calculated. All data were analyzed using the ABI PRISM
567 SDS 2.0 software (Perkin-Elmer). The expression of genes was normalized to the
568 GAPDH gene. The PCR primers were listed in supplementary file 1.

569 **Chromatin immunoprecipitation (ChIP) assay.**

570 ChIP was performed as previously described (Yuan et al., 2015). The following
571 primers were used: Primers: STK38 (5'-CAGCAAGCAACTCACCAGAG-3',
572 5'-TCCTGTTGTCCTCACCCGTA-3'), BMPR2
573 (5'-TTTGTGTCTGGTCTGCTCGG-3', 5'-GCACTTCCAGTGGCTCCG-3'). The
574 percentage of immunoprecipitated DNA relative to the input was calculated and is
575 shown as the mean ± SD from three independent experiments.

576 **Luciferase Assay**

577 To generate the pGl3-STK38-P luciferase reporter,1.2 kb of DNA upstream the
578 STK38 TTS promoter region with ZNF611 binding motif was amplified by
579 polymerase chain reaction (PCR) and cloned into the Firefly luciferase reporter
580 plasmid pGL3-Basic (Promega) using KPN1 and XHO1 restriction sites.0.7 kb of
581 DNA upstream the STK38 TTS promoter region without ZNF611 binding motif was
582 cloned into pGL3-Basic using same restriction sites to generate the pGl3-STK38-ΔP
583 luciferase reporter. HEK293T cells seeded on 48-well plates were incubated until 60%
584 to 70% confluence and then were transient transfected with 0.01 μg pGL3-STK38
585 plasmid using Lipofectamine 2000 (Invitrogen, CA, USA). After transfection 36-48 h,
586 cell lysates were collected for Luciferase activity determination by Dual Luciferase
587 Reporter assay systems (Promega). According to the manufacturer's instructions,
588 luciferase activity was normalized by Renilla activity to standardize transfection
589 efficiency.

590 **Authors' contributions**

591 DY conceived, designed the study, revised the manuscript and supported the
592 funding needed in this study. CT designed the experiments, partly supported the
593 funding needed in this study and partly wrote the manuscript. FH partly designed the
594 study, gave valuable suggestions, and partly supported the funding needed in this
595 study. PS designed, carried out most of the analyses, and wrote the draft manuscript.
596 QZ performed most of the experiments, and partly wrote the draft manuscript. AX,
597 CG, YH participated in part of analyses. JL participated in part of experiments. All
598 authors read and approved the final manuscript.

599 **Acknowledgements**

600 Thanks for the support and help of bioinformatics platform of National Center for
601 Protein Sciences (Beijing) in omics data processing.

602 **Competing interests**

603 The authors declare that they have no competing interests.

604 **References**

605 Baudat, F., Buard, J., Grey, C., Fledel-Alon, A., Ober, C., Przeworski, M., . . . de
606 Massy, B. (2010). PRDM9 is a major determinant of meiotic recombination
607 hotspots in humans and mice. *Science, 327*(5967), 836-840.
608 doi:10.1126/science.1183439
609 Behringer, R. R., Eakin, G. S., & Renfree, M. B. (2006). Mammalian diversity:
610 gametes, embryos and reproduction. *Reprod Fertil Dev, 18*(1-2), 99-107.
611 doi:10.1071/rd05137
612 Birtle, Z., & Ponting, C. P. (2006). Meisetz and the birth of the KRAB motif.
613 *Bioinformatics, 22*(23), 2841-2845. doi:10.1093/bioinformatics/btl498
614 Cardoso-Moreira, M., Halbert, J., Valloton, D., Velten, B., Chen, C., Shao, Y., . . .
615 Kaessmann, H. (2019). Gene expression across mammalian organ
616 development. *Nature, 571*(7766), 505-509. doi:10.1038/s41586-019-1338-5
617 Cassa, C. A., Weghorn, D., Balick, D. J., Jordan, D. M., Nusinow, D., Samocha, K.
618 E., . . . Sunyaev, S. R. (2017). Estimating the selective effects of heterozygous
619 protein-truncating variants from human exome data. *Nature Genetics, 49*(5),
620 806-810. doi:10.1038/ng.3831
621 Chen, W., Schwalie, P. C., Pankevich, E. V., Gubelmann, C., Raghav, S. K., Dainese,
622 R., . . . Deplancke, B. (2019). ZFP30 promotes adipogenesis through the

623 KAP1-mediated activation of a retrotransposon-derived Pparg2 enhancer. *Nat*
624 *Commun, 10*(1), 1809. doi:10.1038/s41467-019-09803-9
625 Consortium, E. P. (2012). An integrated encyclopedia of DNA elements in the human
626 genome. *Nature, 489*(7414), 57-74. doi:10.1038/nature11247
627 Csizmok, V., Follis, A. V., Kriwacki, R. W., & Forman-Kay, J. D. (2016). Dynamic
628 Protein Interaction Networks and New Structural Paradigms in Signaling.
629 *Chem Rev, 116*(11), 6424-6462. doi:10.1021/acs.chemrev.5b00548
630 Dickinson, M. E., Flenniken, A. M., Ji, X., Teboul, L., Wong, M. D., White, J. K., . . .
631 Murray, S. A. (2016). High-throughput discovery of novel developmental
632 phenotypes. *Nature, 537*(7621), 508-514. doi:10.1038/nature19356
633 Dosztanyi, Z. (2018). Prediction of protein disorder based on IUPred. *Protein Sci,*
634 *27*(1), 331-340. doi:10.1002/pro.3334
635 Ecco, G., Cassano, M., Kauzlaric, A., Duc, J., Coluccio, A., Offner, S., . . . Trono, D.
636 (2016). Transposable Elements and Their KRAB-ZFP Controllers Regulate
637 Gene Expression in Adult Tissues. *Dev Cell, 36*(6), 611-623.
638 doi:10.1016/j.devcel.2016.02.024
639 Ecco, G., Imbeault, M., & Trono, D. (2017). KRAB zinc finger proteins. *Development,*
640 *144*(15), 2719-2729. doi:10.1242/dev.132605
641 Eddy, S. R. (2009). A new generation of homology search tools based on probabilistic
642 inference. *Genome Inform, 23*(1), 205-211.
643 Emerson, R. O., & Thomas, J. H. (2009). Adaptive evolution in zinc finger
644 transcription factors. *PLoS Genet, 5*(1), e1000325.
645 doi:10.1371/journal.pgen.1000325
646 Enomoto, A., Kido, N., Ito, M., Morita, A., Matsumoto, Y., Takamatsu, N., . . .
647 Miyagawa, K. (2008). Negative regulation of MEKK1/2 signaling by
648 serine-threonine kinase 38 (STK38). *Oncogene, 27*(13), 1930-1938.
649 doi:10.1038/sj.onc.1210828
650 Feng, J., Liu, T., Qin, B., Zhang, Y., & Liu, X. S. (2012). Identifying ChIP-seq
651 enrichment using MACS. *Nat Protoc, 7*(9), 1728-1740.
652 doi:10.1038/nprot.2012.101
653 Finn, R. D., Mistry, J., Tate, J., Coggill, P., Heger, A., Pollington, J. E., . . . Bateman,
654 A. (2010). The Pfam protein families database. *Nucleic Acids Res,*
655 *38*(Database issue), D211-222. doi:10.1093/nar/gkp985
656 Grey, C., Barthes, P., Chauveau-Le Friec, G., Langa, F., Baudat, F., & de Massy, B.
657 (2011). Mouse PRDM9 DNA-binding specificity determines sites of histone
658 H3 lysine 4 trimethylation for initiation of meiotic recombination. *PLoS Biol,*
659 *9*(10), e1001176. doi:10.1371/journal.pbio.1001176
660 Grey, C., Baudat, F., & de Massy, B. (2018). PRDM9, a driver of the genetic map.
661 *PLoS Genet, 14*(8), e1007479. doi:10.1371/journal.pgen.1007479
662 Guo, Y., Zhang, X., Huang, J., Zeng, Y., Liu, W., Geng, C., . . . He, F. (2009).
663 Relationships between hematopoiesis and hepatogenesis in the midtrimester
664 fetal liver characterized by dynamic transcriptomic and proteomic profiles.

PLoS One, 4(10), e7641. doi:10.1371/journal.pone.0007641

Hamilton, A. T., Huntley, S., Tran-Gyamfi, M., Baggott, D. M., Gordon, L., & Stubbs, L. (2006). Evolutionary expansion and divergence in the ZNF91 subfamily of primate-specific zinc finger genes. *Genome Res, 16*(5), 584-594. doi:10.1101/gr.4843906

Helleboid, P. Y., Heusel, M., Duc, J., Piot, C., Thorball, C. W., Coluccio, A., . . . Trono, D. (2019). The interactome of KRAB zinc finger proteins reveals the evolutionary history of their functional diversification. *EMBO J*, e101220. doi:10.15252/embj.2018101220

Herrero, J., Muffato, M., Beal, K., Fitzgerald, S., Gordon, L., Pignatelli, M., . . . Flicek, P. (2016). Ensembl comparative genomics resources. *Database (Oxford), 2016*. doi:10.1093/database/baw053

Huntley, S., Baggott, D. M., Hamilton, A. T., Tran-Gyamfi, M., Yang, S., Kim, J., . . . Stubbs, L. (2006). A comprehensive catalog of human KRAB-associated zinc finger genes: insights into the evolutionary history of a large family of transcriptional repressors. *Genome Res, 16*(5), 669-677. doi:10.1101/gr.4842106

Imbeault, M., Helleboid, P. Y., & Trono, D. (2017). KRAB zinc-finger proteins contribute to the evolution of gene regulatory networks. *Nature, 543*(7646), 550-554. doi:10.1038/nature21683

Jacobs, F. M., Greenberg, D., Nguyen, N., Haeussler, M., Ewing, A. D., Katzman, S., . . . Haussler, D. (2014). An evolutionary arms race between KRAB zinc-finger genes ZNF91/93 and SVA/L1 retrotransposons. *Nature, 516*(7530), 242-245. doi:10.1038/nature13760

Jurka, J. (2000). Repbase update: a database and an electronic journal of repetitive elements. *Trends Genet, 16*(9), 418-420.

Kang, S., Akerblad, P., Kiviranta, R., Gupta, R. K., Kajimura, S., Griffin, M. J., . . . Rosen, E. D. (2012). Regulation of early adipose commitment by Zfp521. *PLoS Biol, 10*(11), e1001433. doi:10.1371/journal.pbio.1001433

Keilwagen, J., Posch, S., & Grau, J. (2019). Accurate prediction of cell type-specific transcription factor binding. *Genome Biol, 20*(1), 9. doi:10.1186/s13059-018-1614-y

Kim, D., Langmead, B., & Salzberg, S. L. (2015). HISAT: a fast spliced aligner with low memory requirements. *Nat Methods, 12*(4), 357-360. doi:10.1038/nmeth.3317

Kinsella, R. J., Kahari, A., Haider, S., Zamora, J., Proctor, G., Spudich, G., . . . Flicek, P. (2011). Ensembl BioMarts: a hub for data retrieval across taxonomic space. *Database (Oxford), 2011*, bar030. doi:10.1093/database/bar030

Kumar, S., Stecher, G., Li, M., Knyaz, C., & Tamura, K. (2018). MEGA X: Molecular Evolutionary Genetics Analysis across Computing Platforms. *Mol Biol Evol, 35*(6), 1547-1549. doi:10.1093/molbev/msy096

Kumar, S., Stecher, G., Suleski, M., & Hedges, S. B. (2017). TimeTree: A Resource

for Timelines, Timetrees, and Divergence Times. *Mol Biol Evol, 34*(7), 1812-1819. doi:10.1093/molbev/msx116

Kummerfeld, S. K., & Teichmann, S. A. (2006). DBD: a transcription factor prediction database. *Nucleic Acids Res, 34*(Database issue), D74-81. doi:10.1093/nar/gkj131

Larkin, M. A., Blackshields, G., Brown, N. P., Chenna, R., McGettigan, P. A., McWilliam, H., . . . Higgins, D. G. (2007). Clustal W and Clustal X version 2.0. *Bioinformatics, 23*(21), 2947-2948. doi:10.1093/bioinformatics/btm404

Li, H., Quang, D., & Guan, Y. (2019). Anchor: trans-cell type prediction of transcription factor binding sites. *Genome Res, 29*(2), 281-292. doi:10.1101/gr.237156.118

Li, X., Ito, M., Zhou, F., Youngson, N., Zuo, X., Leder, P., & Ferguson-Smith, A. C. (2008). A maternal-zygotic effect gene, Zfp57, maintains both maternal and paternal imprints. *Dev Cell, 15*(4), 547-557. doi:10.1016/j.devcel.2008.08.014

Liu, F., Ventura, F., Doody, J., & Massague, J. (1995). Human type II receptor for bone morphogenic proteins (BMPs): extension of the two-kinase receptor model to the BMPs. *Mol Cell Biol, 15*(7), 3479-3486. doi:10.1128/mcb.15.7.3479

Looman, C., Abrink, M., Mark, C., & Hellman, L. (2002). KRAB zinc finger proteins: an analysis of the molecular mechanisms governing their increase in numbers and complexity during evolution. *Mol Biol Evol, 19*(12), 2118-2130. doi:10.1093/oxfordjournals.molbev.a004037

Ludwig, T. E., Bergendahl, V., Levenstein, M. E., Yu, J., Probasco, M. D., & Thomson, J. A. (2006). Feeder-independent culture of human embryonic stem cells. *Nat Methods, 3*(8), 637-646. doi:10.1038/nmeth902

Mosca, R., Pache, R. A., & Aloy, P. (2012). The role of structural disorder in the rewiring of protein interactions through evolution. *Mol Cell Proteomics, 11*(7), M111 014969. doi:10.1074/mcp.M111.014969

Najafabadi, H. S., Albu, M., & Hughes, T. R. (2015). Identification of C2H2-ZF binding preferences from ChIP-seq data using RCADE. *Bioinformatics, 31*(17), 2879-2881. doi:10.1093/bioinformatics/btv284

Nowick, K., Carneiro, M., & Faria, R. (2013). A prominent role of KRAB-ZNF transcription factors in mammalian speciation? *Trends Genet, 29*(3), 130-139. doi:10.1016/j.tig.2012.11.007

Nowick, K., Fields, C., Gernat, T., Caetano-Anolles, D., Kholina, N., & Stubbs, L. (2011). Gain, loss and divergence in primate zinc-finger genes: a rich resource for evolution of gene regulatory differences between species. *PLoS One, 6*(6), e21553. doi:10.1371/journal.pone.0021553

Oleksiewicz, U., Gladych, M., Raman, A. T., Heyn, H., Mereu, E., Chlebanowska, P., . . . Wiznerowicz, M. (2017). TRIM28 and Interacting KRAB-ZNFs Control Self-Renewal of Human Pluripotent Stem Cells through Epigenetic Repression of Pro-differentiation Genes. *Stem Cell Reports, 9*(6), 2065-2080.

749 doi:10.1016/j.stemcr.2017.10.031
750 Patel, A., Yang, P., Tinkham, M., Pradhan, M., Sun, M. A., Wang, Y., . . . Cheng, X.
751 (2018). DNA Conformation Induces Adaptable Binding by Tandem Zinc
752 Finger Proteins. *Cell, 173*(1), 221-233 e212. doi:10.1016/j.cell.2018.02.058
753 Patro, R., Duggal, G., Love, M. I., Irizarry, R. A., & Kingsford, C. (2017). Salmon
754 provides fast and bias-aware quantification of transcript expression. *Nat*
755 *Methods, 14*(4), 417-419. doi:10.1038/nmeth.4197
756 Pontis, J., Planet, E., Offner, S., Turelli, P., Duc, J., Coudray, A., . . . Trono, D. (2019).
757 Hominoid-Specific Transposable Elements and KZFPs Facilitate Human
758 Embryonic Genome Activation and Control Transcription in Naive Human
759 ESCs. *Cell Stem Cell, 24*(5), 724-735 e725. doi:10.1016/j.stem.2019.03.012
760 Ravasi, T., Suzuki, H., Cannistraci, C. V., Katayama, S., Bajic, V. B., Tan, K., . . .
761 Hayashizaki, Y. (2010). An atlas of combinatorial transcriptional regulation in
762 mouse and man. *Cell, 140*(5), 744-752. doi:10.1016/j.cell.2010.01.044
763 Riso, V., Cammisa, M., Kukreja, H., Anvar, Z., Verde, G., Sparago, A., . . . Riccio, A.
764 (2016). ZFP57 maintains the parent-of-origin-specific expression of the
765 imprinted genes and differentially affects non-imprinted targets in mouse
766 embryonic stem cells. *Nucleic Acids Res, 44*(17), 8165-8178.
767 doi:10.1093/nar/gkw505
768 Schmitges, F. W., Radovani, E., Najafabadi, H. S., Barazandeh, M., Campitelli, L. F.,
769 Yin, Y., . . . Hughes, T. R. (2016). Multiparameter functional diversity of
770 human C2H2 zinc finger proteins. *Genome Res, 26*(12), 1742-1752.
771 doi:10.1101/gr.209643.116
772 Soneson, C., Love, M. I., & Robinson, M. D. (2015). Differential analyses for
773 RNA-seq: transcript-level estimates improve gene-level inferences. *F1000Res,*
774 *4*, 1521. doi:10.12688/f1000research.7563.2
775 Takahashi, N., Coluccio, A., Thorball, C. W., Planet, E., Shi, H., Offner, S., . . . Trono,
776 D. (2019). ZNF445 is a primary regulator of genomic imprinting. *Genes Dev,*
777 *33*(1-2), 49-54. doi:10.1101/gad.320069.118
778 Thomas, J. H., & Schneider, S. (2011). Coevolution of retroelements and tandem zinc
779 finger genes. *Genome Res, 21*(11), 1800-1812. doi:10.1101/gr.121749.111
780 Thurman, R. E., Rynes, E., Humbert, R., Vierstra, J., Maurano, M. T., Haugen, E., . . .
781 Stamatoyannopoulos, J. A. (2012). The accessible chromatin landscape of the
782 human genome. *Nature, 489*(7414), 75-82. doi:10.1038/nature11232
783 Tsankov, A. M., Gu, H., Akopian, V., Ziller, M. J., Donaghey, J., Amit, I., . . .
784 Meissner, A. (2015). Transcription factor binding dynamics during human ES
785 cell differentiation. *Nature, 518*(7539), 344-349. doi:10.1038/nature14233
786 Vilella, A. J., Severin, J., Ureta-Vidal, A., Heng, L., Durbin, R., & Birney, E. (2009).
787 EnsemblCompara GeneTrees: Complete, duplication-aware phylogenetic trees
788 in vertebrates. *Genome Res, 19*(2), 327-335. doi:10.1101/gr.073585.107
789 Watanabe, K., Ueno, M., Kamiya, D., Nishiyama, A., Matsumura, M., Wataya, T., . . .
790 Sasai, Y. (2007). A ROCK inhibitor permits survival of dissociated human

791 embryonic stem cells. *Nat Biotechnol, 25*(6), 681-686. doi:10.1038/nbt1310
792 Wolf, D., & Goff, S. P. (2009). Embryonic stem cells use ZFP809 to silence retroviral
793 DNAs. *Nature, 458*(7242), 1201-1204. doi:10.1038/nature07844
794 Wolf, G., Yang, P., Fuchtbauer, A. C., Fuchtbauer, E. M., Silva, A. M., Park, C., . . .
795 Macfarlan, T. S. (2015). The KRAB zinc finger protein ZFP809 is required to
796 initiate epigenetic silencing of endogenous retroviruses. *Genes Dev, 29*(5),
797 538-554. doi:10.1101/gad.252767.114
798 Yang, D., Ma, Z., Lin, W., Yang, J., Tian, C., Wei, H., . . . He, F. (2013). Identification
799 of KAP-1-associated complexes negatively regulating the Ey and beta-major
800 globin genes in the beta-globin locus. *J Proteomics, 80C*, 132-144.
801 doi:10.1016/j.jprot.2012.12.014
802 Yang, D., Zhong, F., Li, D., Liu, Z., Wei, H., Jiang, Y., & He, F. (2012). General
803 trends in the utilization of structural factors contributing to biological
804 complexity. *Mol Biol Evol, 29*(8), 1957-1968. doi:10.1093/molbev/mss064
805 Yang, P., Wang, Y., & Macfarlan, T. S. (2017). The Role of KRAB-ZFPs in
806 Transposable Element Repression and Mammalian Evolution. *Trends Genet,*
807 *33*(11), 871-881. doi:10.1016/j.tig.2017.08.006
808 Yuan, L., Chen, Z., Song, S., Wang, S., Tian, C., Xing, G., . . . Zhang, L. (2015). p53
809 degradation by a coronavirus papain-like protease suppresses type I interferon
810 signaling. *J Biol Chem, 290*(5), 3172-3182. doi:10.1074/jbc.M114.619890
811 Zerbino, D. R., Achuthan, P., Akanni, W., Amode, M. R., Barrell, D., Bhai, J., . . .
812 Flicek, P. (2018). Ensembl 2018. *Nucleic Acids Res, 46*(D1), D754-D761.
813 doi:10.1093/nar/gkx1098
814 Zhang, Y., Liu, T., Meyer, C. A., Eeckhoute, J., Johnson, D. S., Bernstein, B. E., . . .
815 Liu, X. S. (2008). Model-based analysis of ChIP-Seq (MACS). *Genome Biol,*
816 *9*(9), R137. doi:10.1186/gb-2008-9-9-r137
817

818

Figure legends

Fig. 1. Comparison of divergence time of full protein sequence, KRAB domain and zinc finger in KZFPs. (*A*) Box plots of the divergence time of full protein sequence, KRAB domain and zinc finger in KZFPs. The values of upper and lower quartiles are indicated as upper and lower edges of the box, and the median values of median are indicated as a bar in the box. The differences of divergence time among gene, KRAB domain and zinc finger are examined by Mann–Whitney U test. The corrected P values are shown in the top of the panel. *(B-D)* Comparison of the three types of divergence time for each KZFP. In each subgraph, there are two dots for every KZFP, representing two types of divergence time. One is above the zero line and the other one is below it. The difference values of the two types of divergence time are shown as broken lines in each subgraph with the right axis as the reference scale. According to the comparison results, KZFPs are divided into three classes for each type of comparison. The numbers and percentages of KZFPs in each class are shown in brackets on the label of X-axis.

Fig. 2. Sequence diversification of KRAB domains and zinc fingers in human KZFPs. (*A*) The phylogenetic tree of KRAB domain A-boxes in human KZFPs associated with their corresponding KRAB domain divergence time and zinc finger divergence time shown as heatmap. The variant KRAB domain cluster (right) also are displayed as a zoom-in in this figure. (*B*) The structural disorder ratio (SDR) values of the variant KRAB domains (vKRAB) and the standard KRAB domains (sKRAB). (*C*) The SDR values of KRAB domains in KZFPs with different divergence time grades of zinc finger. (*D*) The similarity values of the key amino acids in zinc fingers of KZFPs. The proportions of the similar zinc fingers (see Method for detail) in each pair KZFPs are defined as the similarity values (0-1) shown in the heatmap. As the number of zinc fingers in two KZFPs can vary significantly, we display the average similarity level. The divergence time of KRAB domain and zinc fingers of each KZFP are shown as heatmap in the bottom of the panel. (*E*) The histogram of similarity values of the key amino acids in zinc fingers of KZFPs between each KZFP pairs. The KZFP pair number and the percentage with similarity values ≥ 0.6 are shown in the figure. (*F*) The gene number and percentage of paralogous gene and

848 singleton in KZFPs. For box-plots (*B*-*C*), the values of upper and lower quartiles are indicated as
849 upper and lower edges of the box, and the median values of median are indicated as a bar in the
850 box. The differences of SDR values between different categories are examined by Mann–Whitney
851 U test. The corrected P values are shown in the top of each panel. The abbreviations in the figure:
852 Am-Th, Amniota-Theria; Eu-Ha, Eutheria-Haplorrhini; Si-Ho, Simiiformes-Homo.

853 **Fig. 3. The tendency of KZFPs binding to non-TE regions and its functional significance.** (*A*)
854 Heatmap showing the percentage of the peaks not overlapping with TE for each KZFP in multiple
855 types of genomics regions. Each row represents a type o genomic region. Each column represents
856 a KZFP. All the KZFPs were classified into seven divergence time grades based on the zinc finger
857 divergence time. The numbers in the left of the panel represent the percentage values of KZFPs
858 not tending to bind to TE in each type of genomic region. (*B*) The binding bias of KZFPs with
859 different zinc finger divergence time grades. The peaks mapping within the whole genome and
860 PCG (protein-coding gene) promoter regions were analyzed. The red dashed line represents 50%.
861 (*C*), The classification of PCGs into three types: noKZFP PCG, KZFP-TE PCG and KZFP-nonTE
862 PCG. noKZFP_PCGs, the PCGs where no KZFP peak binds to their promoters; KZFP-TE_PCGs,
863 the PCGs where at least one KZFP peak binds to TEs in their promoters; KZFP-nonTE_PCGs, the
864 PCGs where at least one KZFP peak binds to their promoters and all KZFP peaks binding to the
865 promoters only bind to non-TE regions. (*D*) Over- or under-representation analysis of biological
866 processes for the three types of PCGs. The over- or under-representation strengths of each class
867 were represented by −log (*p*) or log (*p*), respectively and were shown in the heat map. (*E*)
868 Comparison of the tolerance to functional variation among the three types of PCGs. (*F*) the
869 comparison of the ratio of nonsynonymous and synonymous distance (dN/dS) among the three
870 types of PCGs. For the box plots (*B, E, F*), the values of upper and lower quartiles are indicated as
871 upper and lower edges of the box, and the median values of median are indicated as a bar in the
872 box.. The differences of expression width between different categories are examined by
873 Mann–Whitney U test. The corrected P values are shown in the top of each panel.

874

875 **Fig. 4. The correlation between the three types of divergence time and the expression level of**
876 **KZFP genes.** (*A*), left, heatmap showing spearman's rank correlation coefficients between the

divergence time of full protein sequence, KRAB domain or zinc finger in KZFPs and the gene expression level; right, heatmap showing the gene expression level which is classified into 4 grades (H, M, L, U). Each column represents a KZFP. All the KZFPs were classified into seven classes according to the divergence time of the zinc fingers. Five types of samples are marked as bars with different colors, including human early embryonic development, three directions of ESC differentiation and adult organs or tissues. (*B*) Zoom-in on the expression level of genes encoding KZFPs with young zinc fingers in early embryo development and early mesoderm differentiation.

Fig. 5. The functions of KZFP target genes in the differentiation of ESC into mesoderm. (*A*) the percentage of KZFP peaks binding to TEs or non-TE regions within accessible chromatin in the genome or PCG promoters in ESCs. (*B*) schematic diagram of the work flow for KZFP target gene screening (See method for detailed description). (*C*) the significantly over- or under-represented biological process terms for the two types of PCGs (KZFP-TE PCGs and KZFP-nonTE PCGs) in the differentiation of ESC into mesoderm. The over- or under-representation strengths of each class were represented by -log (*p*) or log (*p*), respectively and were shown in the heat map. (*D*) the tolerance to functional variants between KZFP-TEs and KZFP-nonTEs in differentiation of ESC into mesoderm. (E) the evolutionary rate of KZFP-TEs and KZFP-nonTEs in differentiation of ESC into mesoderm. For the box plots (*D&E*), the values of upper and lower quartiles are indicated as upper and lower edges of the box, and the median values of median are indicated as a bar in the box. The differences of the tolerance to functional variation and the evolutionary rate between different categories are examined by Mann–Whitney U test. The corrected P values are shown in the top of each panel.

Fig. 6. The regulatory and co-evolution relationship between ZNF611, a KZFP containing young zinc fingers, and STK38, one of its target genes in ESCs. (A) Effect of ZNF611 overexpression on the mRNA level of its target genes. Total RNA from ZNF611 transfected ESC cells was subjected to real-time quantitative PCR (qPCR) analysis. Control: empty vector. (B) Effect of ZNF611 knockdown on the mRNA level of its target genes. For panel A and B, relative

mRNA levels of predicted target genes were normalized to GAPDH. The ratio values (relative expression level / the averdivergence time control value) were shown. Data are means ± SD (n = 3). The differences of expression level between control and KZFP overexpression are assessed by t-test. **: $p < 0.01$, *: $p < 0.05$. (C) Screenshot of ZNF611 binding sites and chromatin accessibility in ESC and mesoderm at genomic loci corresponding to STK38. (D) ESCs were transfected with empty vectors or Flag-tagged ZNF611 expression plasmids. After 36 h, cells were harvested and ChIP assay was performed using antibodies against IgG or Flag, and quantitative PCR was performed with primer sets against STK38 target promoters, indicating ZNF611 occupancy. Data are represented as means ± S.D. (n = 3). All data present results from three independent experiments. (E) the molecular phylogenetic tree of key amino acids in zinc fingers of ZNF611 in Simiiformes. The percentage of replicate trees in which the associated taxa clustered together in the bootstrap test (2000 replicates) are shown next to the branches. The evolutionary distances were computed using the Poisson correction method and are in the units of the number of amino acid substitutions per site. (F) ZNF611 binding motif predicted by RACDE. (G) Alignment of the STK38 promoter locus from 21 representative species. (H) Schematic representation of STK38 promoter reporter plasmids with or without ZNF611 binding site. (I) HEK293T cells were transfected with STK38 promoter reporter plasmids, and luciferase activities were measured and normalized. Representative results of three independent reporter assay experiments are shown. The data are represented as the mean ± S.D. (n = 3). All data present results from three independent experiments. pGL3-STK38-P: full construct; pGL3-STK38-ΔP: ZNF611 binding motif deletion.

Fig. 7. The ′two-way model′ of KZFP family evolution. The evolution of the KZFP family is mainly divided into two directions. One is the divergence of key amino acids in the zinc fingers (zinc finger array varied). In another evolutionary path, the key amino acids in the zinc fingers are conserved, but the sequence of KRAB domain is diverged (KRAB domain varied).

Figure 1

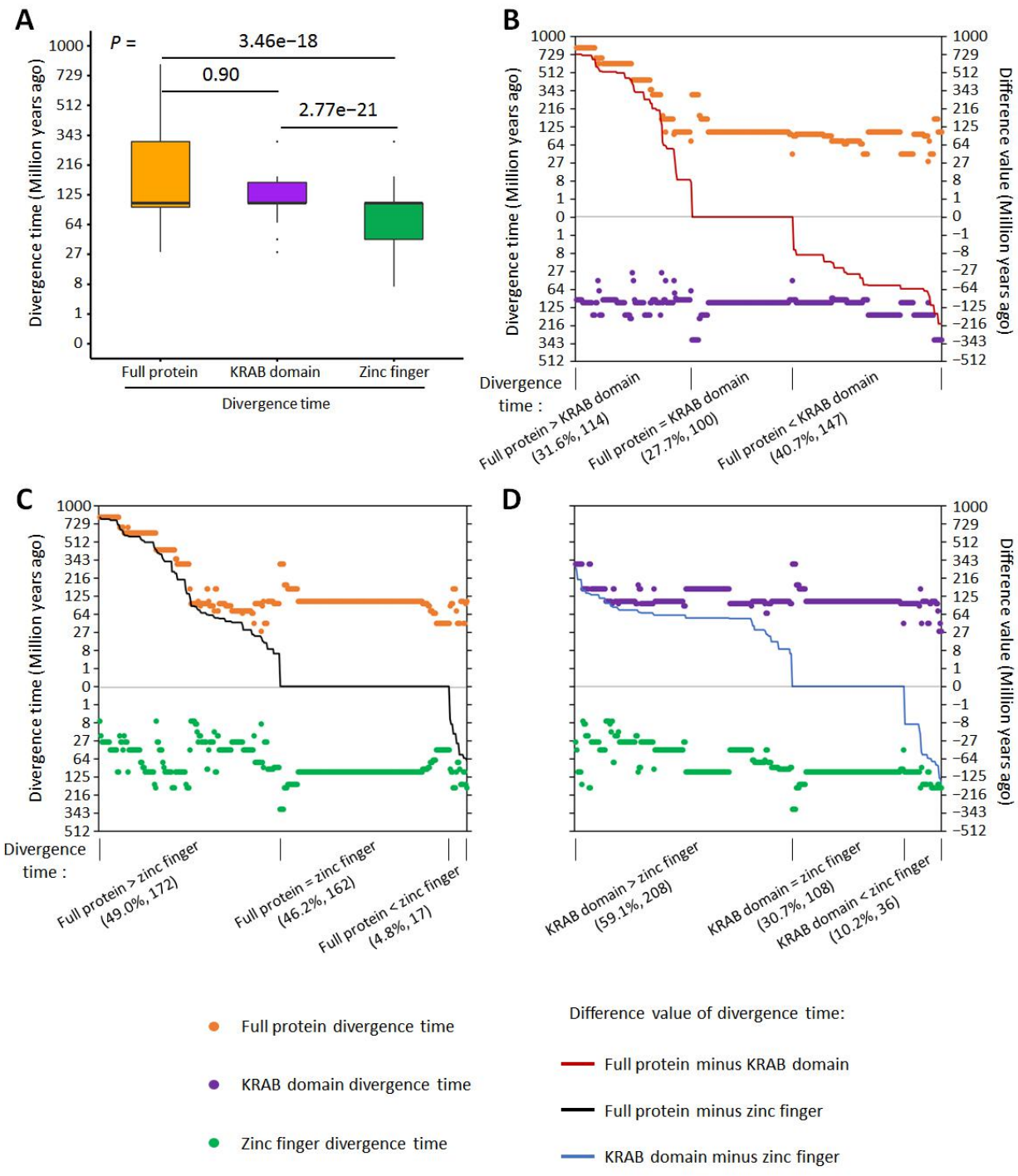

Figure 2

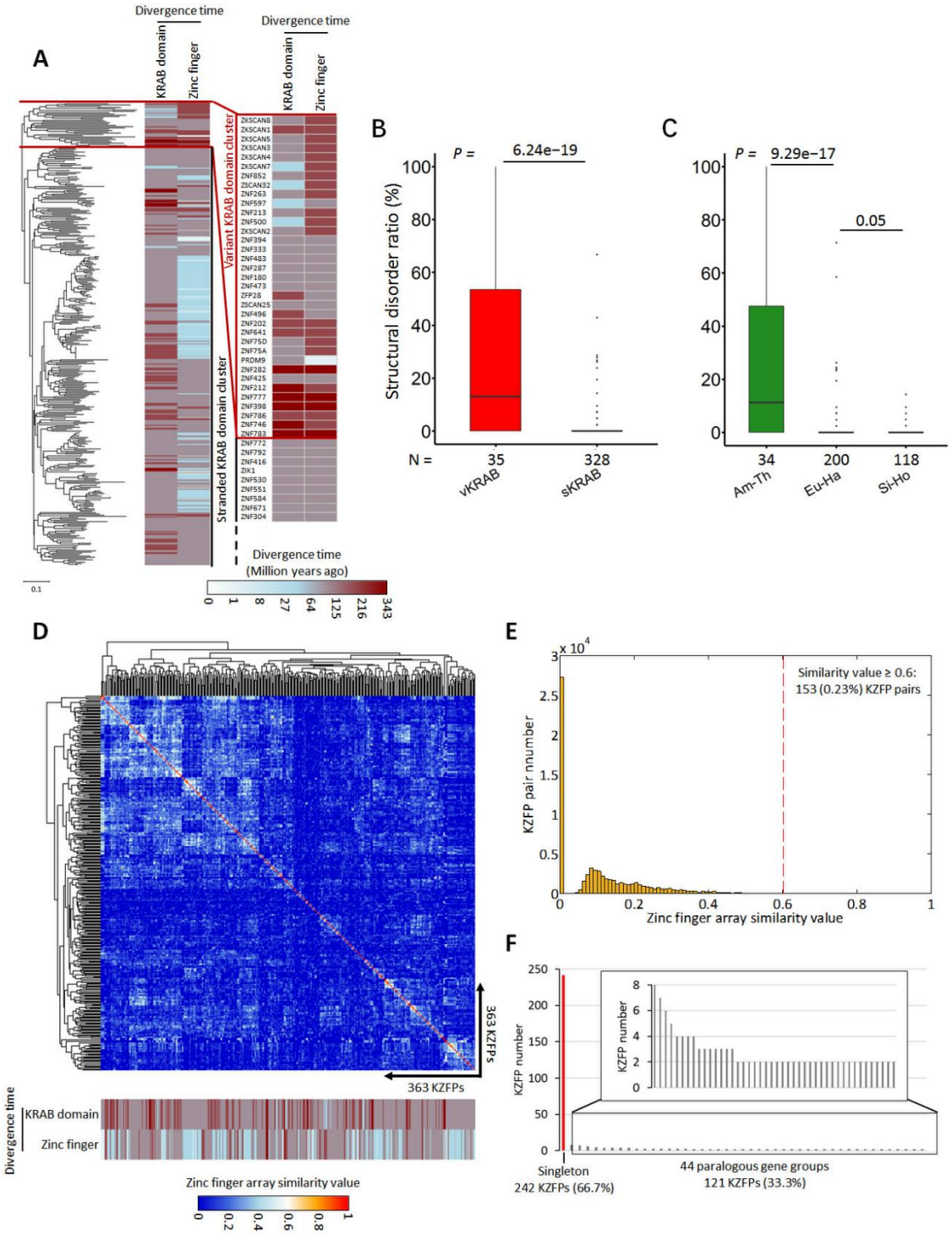

Figure 3

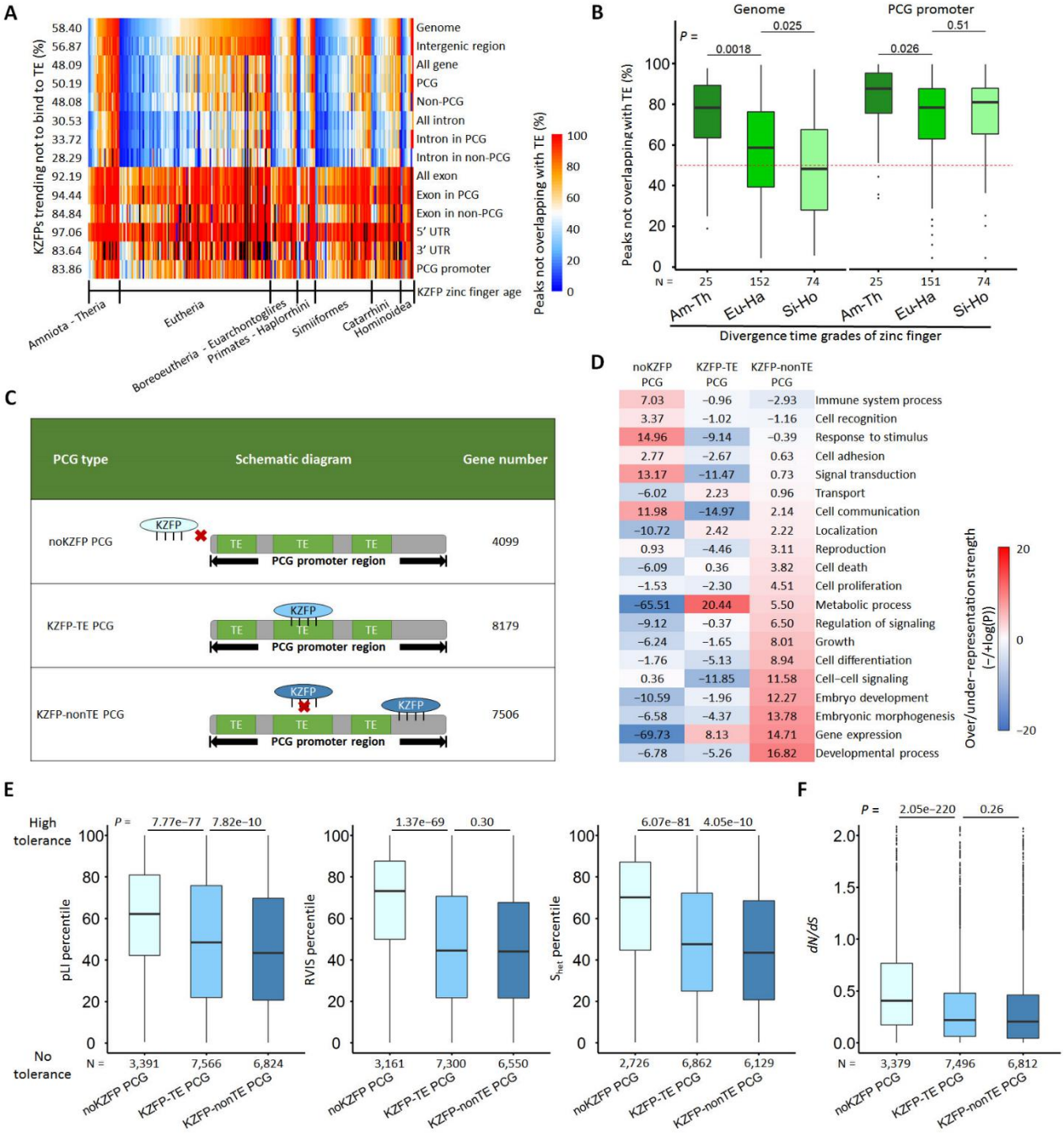

Figure 4

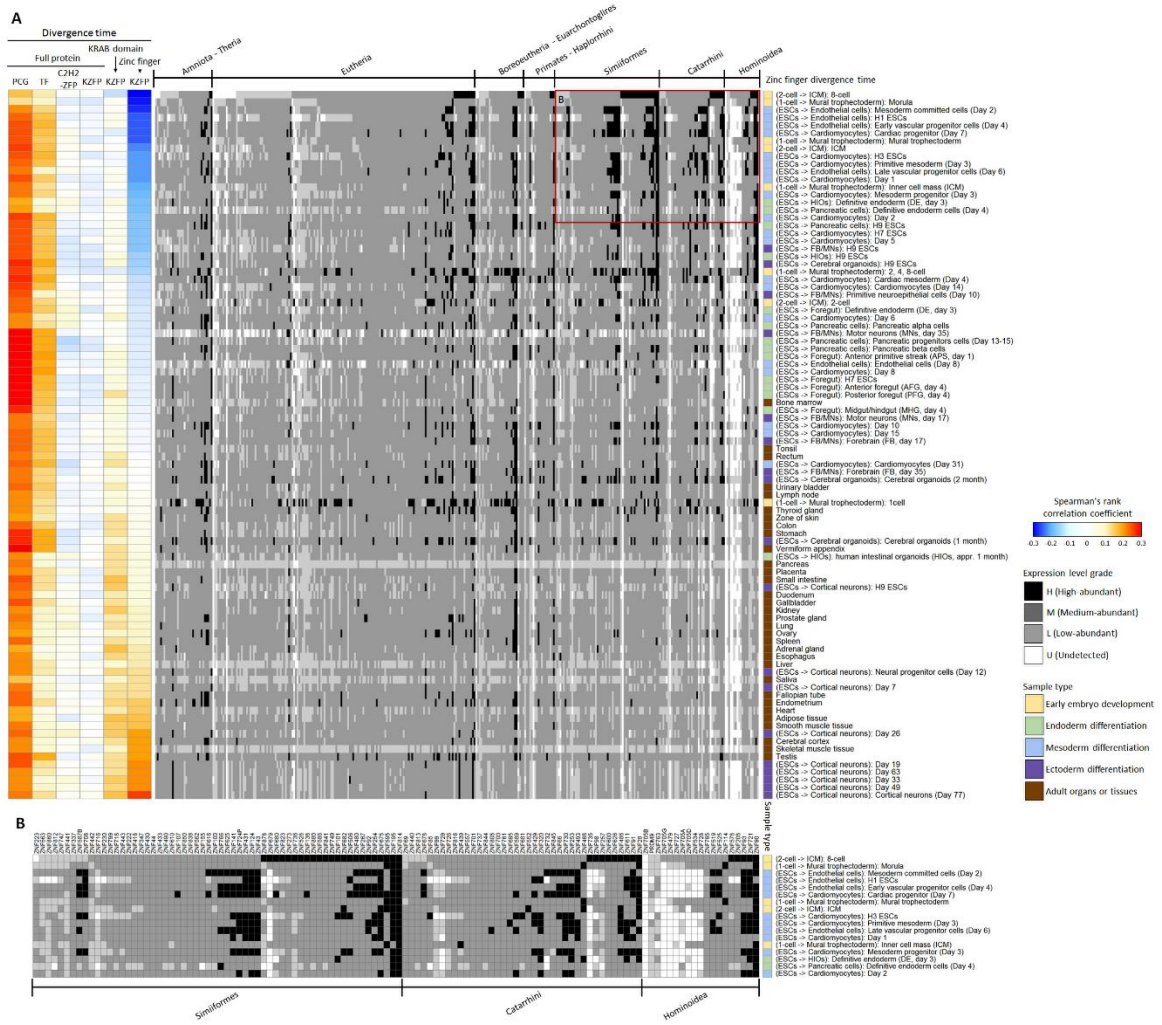

Figure 5

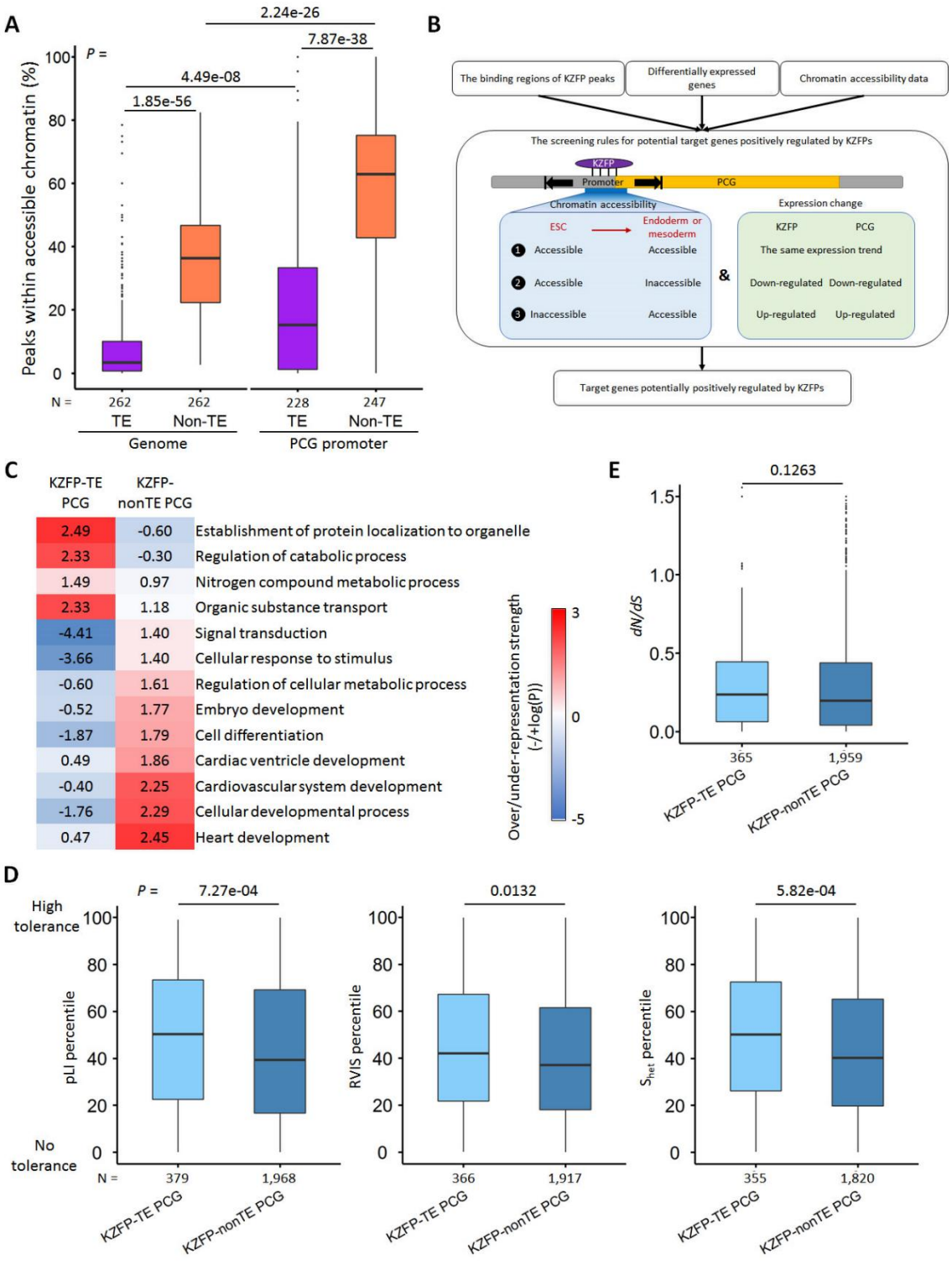

Figure 6

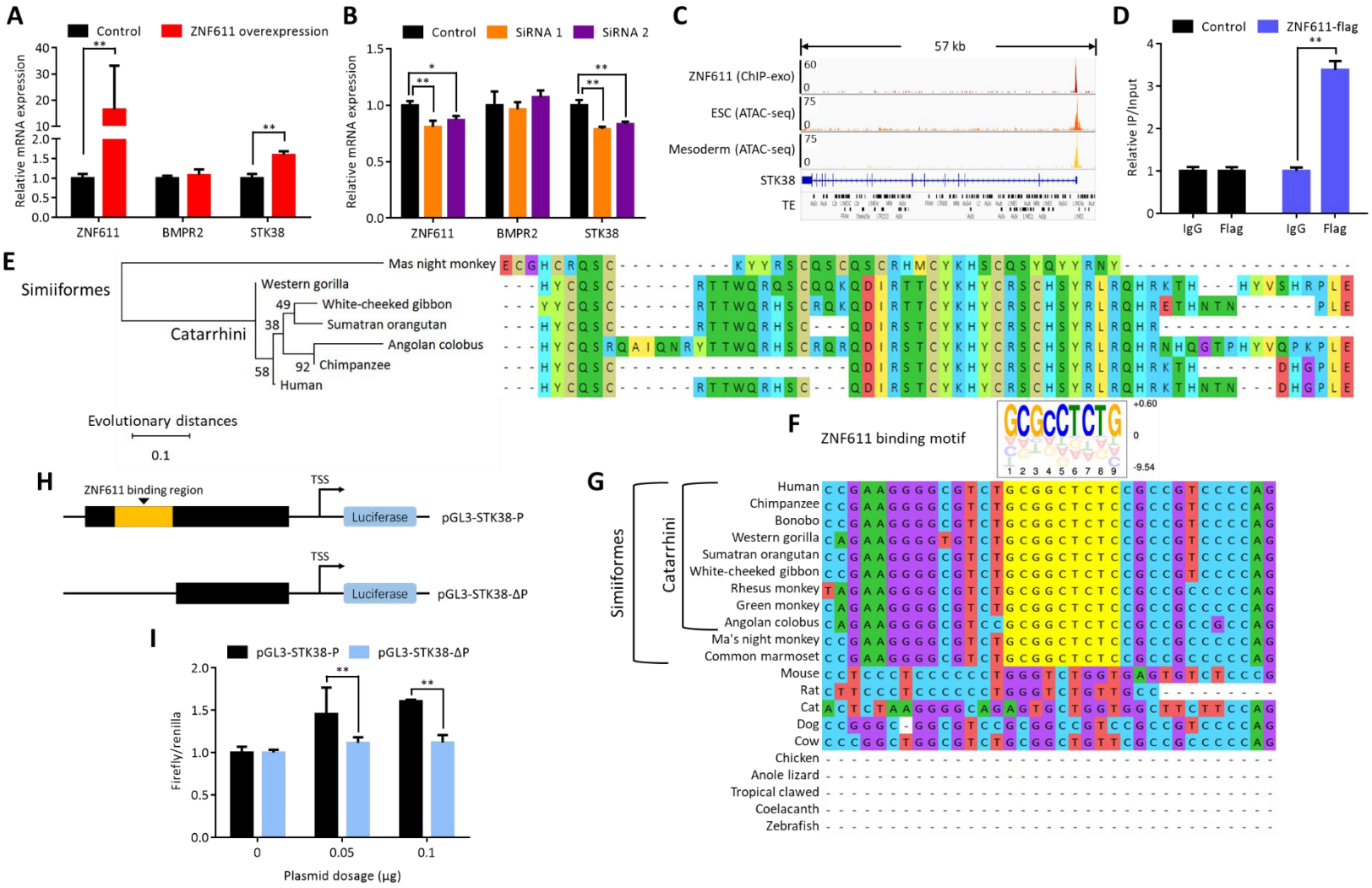
A
Control
ZNF611 overexpression
Relative mRNA expression
ZNF611
BMPR2
STK38
B
Control
SiRNA 1
SiRNA 2
Relative mRNA expression
ZNF611
BMPR2
STK38
C
57 kb
ZNF611 (ChIP-exo)
ESC (ATAC-seq)
Mesoderm (ATAC-seq)
STK38
TE
D
Control
ZNF611-flag
Relative IP/Input
IgG
Flag
IgG
Flag
E
Simiiformes
Catarrhini
Western gorilla
White-cheeked gibbon
Sumatran orangutan
Angolan colobus
Chimpanzee
Human
Mas night monkey
Evolutionary distances
0.1
F
ZNF611 binding motif
G
Simiiformes
Catarrhini
Human
Chimpanzee
Bonobo
Western gorilla
Sumatran orangutan
White-cheeked gibbon
Rhesus monkey
Green monkey
Angolan colobus
Ma's night monkey
Common marmoset
Mouse
Rat
Cat
Dog
Cow
Chicken
Anole lizard
Tropical clawed
Coelacanth
Zebrafish
H
ZNF611 binding region
TSS
Luciferase
pGL3-STK38-P
TSS
Luciferase
pGL3-STK38-ΔP
I
pGL3-STK38-P
pGL3-STK38-ΔP
Firefly/renilla
Plasmid dosage (μg)

Figure 7

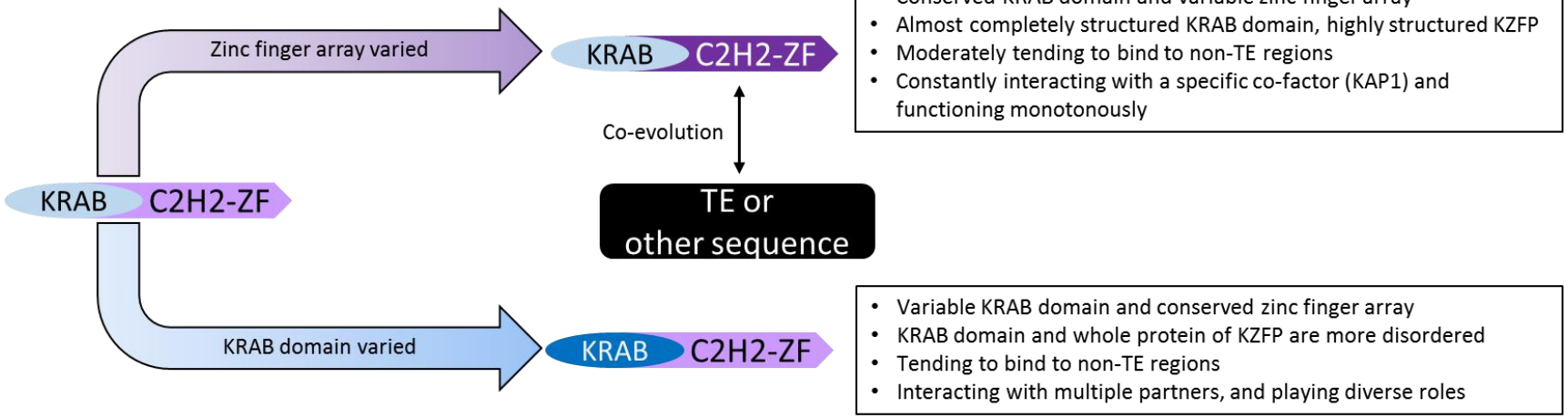
Zinc finger array varied
KRAB
C2H2-ZF
Co-evolution
TE or other sequence
KRAB
C2H2-ZF
KRAB domain varied
KRAB
C2H2-ZF
• Conserved KRAB domain and variable zinc finger array
• Almost completely structured KRAB domain, highly structured KZFP
• Moderately tending to bind to non-TE regions
• Constantly interacting with a specific co-factor (KAP1) and functioning monotonously
• Variable KRAB domain and conserved zinc finger array
• KRAB domain and whole protein of KZFP are more disordered
• Tending to bind to non-TE regions
• Interacting with multiple partners, and playing diverse roles